

proliferative membranes of patients with diabetic retinopathy. The level of vasohibin-1 is significantly correlated with the VEGF level in the vitreous of patients with proliferative diabetic retinopathy.<sup>17</sup> Vasohibin-1 is also expressed in the CNV membranes of patients with AMD.<sup>18</sup> Eyes with lower vasohibin-1/VEGF expression ratios tend to have larger CNV lesions, whereas those with higher vasohibin-1/VEGF ratios have subretinal fibrosislike lesions.<sup>18</sup>

We have found that the laser-induced CNVs were less active in mice injected intravitreally with vasohibin-1 than those injected with the vehicle.<sup>19</sup> Thus, the purpose of this study was to determine the effect of intravitreal vasohibin-1 on the laser-induced CNVs in monkey eyes. We shall show that the intravitreal vasohibin-1 was safe and reduced the degree of the CNVs in monkey eyes.

## Methods

### Animals

The procedures used in the animal experiments followed the guidelines of the The Association for Research in Vision and Ophthalmology Statement for the Use of Animals in Ophthalmic and Vision Research, and they were approved by the Animal Care Committee of Tohoku University Graduate School of Medicine. Twelve Japanese macaque monkeys (*Macaca fuscata*) between ages 4 and 6 years and weighing between 4.2 kg and 10.1 kg were used (Table 1). For all procedures, the monkeys were anesthetized with an intramuscular injection of ketamine hydrochloride (35 mg/kg) and xylazine hydrochloride (5 mg/kg), and the pupils were dilated with topical 2.5% phenylephrine and 1% tropicamide. Oxybuprocaine hydrochloride (0.4%) was also used for local anesthesia. Three monkeys were

From the \*Division of Clinical Cell Therapy, United Center for Advanced Medical Research and Development; †Department of Ophthalmology and Visual Science, Graduate School of Medicine, Tohoku University, Miyagi, Japan; ‡Department of Ophthalmology, Iwate Medical University, Iwate, Japan; §Diagnostic Division, Shionogi & Co., Ltd. Osaka, Japan; and ¶Department of Vascular Biology, Institute of Development, Aging, and Cancer, Tohoku University Graduate School of Medicine, Miyagi, Japan.

Supported in part by grants from Grants-in-Aid for Scientific Research 21592214 and 20592030 (to T. Abe) from the Japan Society for the Promotion of Science, Chiyoda-ku, Tokyo, Japan and by Suzuken Memorial Foundation.

This study was performed at the Tohoku University. Monkeys were supplied by National BioResource Project for breeding and supply.

The authors declare no conflict of interest.

Reprint requests: Toshiaki Abe, MD, Division of Clinical Cell Therapy, United Center for Advanced Research and Translational Medicine (ART), Graduate School of Medicine, Tohoku University, 1-1 Seiryomachi Aobaku Sendai, Miyagi, 980-8574 Japan; e-mail: toshi@oph.med.tohoku.ac.jp

Table 1. Monkey Eyes Used in This Study

	Vasohibin (mg)	Number of Eyes	Inflammation
Nontreated	0	1	0/1
	0.01	1	0/1
	0.1	1	0/1
	1	1	0/1
	10	1	1/1
	100	1	1/1
Laser application	0	3	0/3
	0.01	3	0/3
	0.1	3	0/3
	1	3	1/3
Laser application	0	3	0/3
	0.1	3	0/3
Total		24	3/24

Inflammation shows clinical inflammation signs that were observed during the experiments.

used to evaluate the safety of intravitreal vasohibin-1, 6 monkeys for dose dependency of a single injection of vasohibin-1, and 3 monkeys for repeated injections of vasohibin-1.

### Experimental Choroidal Neovascularization

An argon green laser was used to rupture of the choroidal membrane using a slit-lamp delivery system (Ultima 2000SE; Lumenis, Yokneam, Israel) with a contact lens.<sup>20</sup> The laser settings were as follows: 50- $\mu$ m diameter, 0.1-second duration, and 650-mW to 750-mW intensity. Five laser burns were made around the macula within 15° of the fovea. The foveola was not treated. Each burn was confirmed to have induced subretinal bubbles indicating a rupture of Bruch membrane.

### Expression and Purification of Human Vasohibin-1 Polypeptide

Human vasohibin-1 was purified from *Escherichia coli* as described.<sup>21</sup> Human vasohibin-1 was isolated as a thioredoxin fusion protein. The fusion protein was dialyzed and digested with blood coagulation Factor Xa (Novagen, Darmstadt, Germany). The released vasohibin-1 was collected, eluted, and dialyzed against 20 mM glycine-HCl buffer (pH 3.5). Then, the vasohibin-1 was resolubilized with 50 mM Tris-HCl buffer containing 50 mM NaCl, 5 mM tris(2-carboxyethyl)phosphine, 0.5 mM ethylenediaminetetraacetic acid, 5% glycerol, and 4.4% *N*-lauroylsarcosine (pH 8.0) and was dialyzed against 20 mM sodium phosphate buffer at pH 8.0. This buffer was also used as the vehicle.

The protein concentration was determined by the Bradford method with a protein assay kit (Bio-Rad Laboratories, Hercules, CA), with bovine serum albumin as a standard protein.

### *Intravitreal Injection of Recombinant Vasohibin-1 Polypeptide*

Vasohibin-1 was injected intravitreally in 3 groups of monkeys (Table 1). The first group of 6 eyes did not have a laser burn and received a single injection of vehicle, or 0.01, 0.1, 1, 10, or 100  $\mu\text{g}$  of vasohibin-1/50  $\mu\text{L}$  of vehicle. The second group of 12 eyes of 6 monkeys (3 eyes for each concentration) received a single injection of vehicle or 0.01, 0.1, and 1  $\mu\text{g}$  of vasohibin-1/50  $\mu\text{L}$  of vehicle 4 days after the laser burn. The third group of 3 eyes had 3 injections of 0.1  $\mu\text{g}$  of vasohibin-1/50  $\mu\text{L}$  of vehicle in the right eyes and 50  $\mu\text{L}$  of vehicle in 3 fellow eyes on 0, 4, and 7 days after the laser burn. We examined the natural course of laser-induced CNVs in mice, and the CNVs were most active around Day 14 after the laser burn, and then gradually regressed, especially 28 days after laser burn. When we injected vasohibin-1 into the vitreous of mice after laser burns, we found that the injection of vasohibin-1 on Day 4 after the laser burn was most effective, followed by Days 7 and 1. Other days were less effective. In addition, immunohistochemical studies for vasohibin-1 in the mouse CNV membranes showed that the later the laser burn, the more vasohibin-1 staining was observed.<sup>19</sup> So we decided to do the repeated vasohibin-1 injections on 0, 4, and 7 days after the laser burn (relatively early days after laser burn).

For the intravitreal injections, the monkeys were anesthetized and pupils were dilated. The intravitreal injections were made with a 30-gauge needle attached to a 1-mL syringe. The needle was inserted through the sclera into the vitreous cavity  $\sim 1.5$  mm posterior to the limbus while observing the eye with an operating microscope. The fundus was examined after the injection to confirm that the retina and lens were not damaged.

### *Ophthalmic Examinations*

In addition to the routine ophthalmologic examinations, fluorescein angiography (FA) with an imaging system (GENESIS-Df; Kowa, Tokyo, Japan), optical coherence tomography (OCT, RS3000; NIDEK, Tokyo, Japan), and focal and full-field electroretinography (ERG) were performed on the selected days. Fluorescein angiography was performed 1, 2, and 4 weeks after the laser photocoagulation. Two retinal specialists (R.W. and T.A.) graded the angiograms in a masked way using a grading system<sup>22</sup>: Grade 1, no hyperfluorescence; Grade 2, hyperfluorescence without leakage; Grade 3, hyperfluorescence in the early or middle phase and leakage in the late phase; and Grade 4, bright

hyperfluorescence in the transit and leakage in late phase beyond the treated areas.

The central macular thickness was determined from the macular thickness maps (3.45 mm in diameter) of the scans by OCT 4 weeks after the laser photocoagulation. The volume of the lesion was also calculated using the same program.

The pupils were maximally dilated for the ERG recordings 4 weeks after intravitreal vasohibin-1 injections. The ERGs were amplified and digitally band-pass filtered from 0.5 Hz to 500 Hz for the full-field ERGs and from 5 Hz to 500 Hz for the focal ERGs (PuREC; Mayo, Aichi, Japan). The animals were dark adapted for at least 30 minutes before the full-field ERG recordings. The light for the stimulus was obtained from light-emitting diodes (EW-102; Mayo Co., Nagoya, Japan) embedded in a contact lens electrode. The intensity and duration of the stimuli were controlled by an electronic stimulator (WLS-20; Mayo Co.). Chlorided silver plate electrodes were placed on the forehead and right ear lobe as reference and ground electrodes, respectively. The intensity of the stimulus was 1,000  $\text{cd}/\text{m}^2$  and the duration was 3 milliseconds.

Focal ERGs were recorded 4 weeks after the laser photocoagulation with a focal ERG system (PuREC; Mayo; ER-80; Kowa) that was integrated into an infrared fundus camera. This system was developed and described in detail by Miyake et al.<sup>23,24</sup> The stimulus spot was 15° in diameter and was placed on the macula by viewing the ocular fundus on a monitor. The intensity of the stimulus was 1,000  $\text{cd}/\text{m}^2$ , and the background light was 1.5  $\text{cd}/\text{m}^2$ . The stimulus duration was 100 milliseconds. A Burian-Allen bipolar contact lens electrode (Hansen Ophthalmic Laboratories, Iowa City, IA) was inserted into the anesthetized conjunctival sac to record the focal ERGs. A chlorided silver electrode was placed on the left ear lobe as the ground electrode. Two hundred to 300 responses were averaged at a stimulation rate of 5 Hz.

The a-waves were measured from the baseline to the trough of the first negative response, and the b-wave from the first trough to the peak of the following positive wave. The amplitudes of a-waves and b-waves from the three untreated monkeys were used as control. The number of monkeys used in this experiment was not added to the total number of monkeys.

### *Immunohistochemistry*

Immunostaining for vasohibin-1 was done on eyes with laser-induced CNVs 28 days after the laser application. From the results of CNV experiments on

mice,<sup>19</sup> the laser-induced CNV lesions were self-resolved >28 days after the laser burn. Thus, we decided to enucleate the eyes 28 days after the laser burn, although there may be differences between mice and monkeys. The eyes were enucleated and fixed in 4% paraformaldehyde overnight, and the anterior segment and lens were removed. The posterior segment was embedded in paraffin, and 3- $\mu$ m serial sections were cut, and adjacent sections were stained with hematoxylin and eosin.

The immunohistochemical staining for vasohibin-1 was performed with the peroxidase method and for cytokeratin by the alkaline phosphatase method. Mouse monoclonal antibodies against vasohibin-1 (1:400) and mouse monoclonal anti-pan cytokeratin (1:200; Sigma-Aldrich, St. Louis, MO) were applied to the sections overnight at 4°C. Then the sections were incubated in biotin-conjugated anti-mouse immunoglobulin (Histfine SAB-PO(M) kit; Nichirei, Tokyo, Japan). The slides for vasohibin were incubated with peroxidase-conjugated streptavidin (Histfine SAB-PO(M) kit; Nichirei), and the slides for cytokeratin were incubated with alkaline phosphatase-conjugated streptavidin (Histfine; Nichirei). HistoGreen (HISTOPRIME HistoGreen substrate kit for peroxidase; Ab Cys SA) was used for the chromogen of vasohibin, and VECTOR RED (alkaline phosphatase substrate kit 1; Vector, Burlingame, CA) was used for the chromogen of cytokeratin. The slides were counterstained with hematoxylin. For control, pre-immune mouse immunoglobulin G was used instead of the primary antibody.

#### *Enzyme-Linked Immunosorbent Assay for Vascular Endothelial Growth Factor*

Aqueous was collected by a 30-gauge needle from the anterior chamber of each monkey 4 weeks after the laser photocoagulation. The level of the VEGF peptide was quantified by enzyme-linked immunosorbent assay according to the manufacturer's instructions (R & D Systems, Mckinley, MN; Quantikine Human VEGF immunoassay) using 50  $\mu$ L of aqueous. The intensity of the color of the reaction products was measured with a MAXline microplate reader (Molecular Devices Corporation, Palo Alto, CA). The measurements were made in duplicate, and the mean was used. The concentration of VEGF was expressed as the amount of protein in picograms per milliliter (pg/mL).

#### *Statistical Analyses*

Analysis of variance with Scheffe test for post hoc analysis was used to examine the differences in the leakage and intensity of the CNVs in the fluorescein angiograms, amplitudes of the ERGs, mean central

thickness, and volume of the CNV. The differences were also compared using the Student two-sample *t*-tests.

## **Results**

### *Safety Evaluations and Outcomes*

Before any of the procedures, the retina and choroid were normal in all the monkeys. Then 6 nontreated eyes were injected intravitreally with vehicle or 0.01, 0.1, 1, 10, or 100  $\mu$ g of vasohibin-1/50  $\mu$ L. After 0.01, 0.1, and 1  $\mu$ g of vasohibin-1, the appearance of the retina and choroid did not differ from that of the vehicle-injected eyes. When 10  $\mu$ g or 100  $\mu$ g/50  $\mu$ L of vasohibin-1 polypeptide was injected, a mild inflammation (Grade 1)<sup>25</sup> was detected in the vitreous on the day after the injection. The inflammation was less with 10  $\mu$ g than with 100  $\mu$ g of vasohibin, and the inflammation was resolved in 2 days after 10  $\mu$ g and in 1 week after 100  $\mu$ g (Table 1). When we injected 1  $\mu$ g/50  $\mu$ L of vasohibin-1 once in the laser-treated eyes, 1 of the 3 eyes developed inflammation in the aqueous. An inflammation was not observed when 0.1  $\mu$ g of vasohibin-1 was injected even after 3 injections. When we injected 50  $\mu$ L of vehicle with almost the same amount of endotoxin (400 U/mL) as that of 100  $\mu$ g of vasohibin-1, no inflammation was detected. These results indicated that mild inflammation can develop with  $\geq 10$   $\mu$ g of vasohibin-1 injection into the vitreous in nontreated monkey eyes.

The amplitudes of the a- and b-waves of the full-field ERGs of eyes injected with 0.01  $\mu$ g to 100  $\mu$ g of vasohibin-1 did not differ significantly from the vehicle-injected eyes. The a-wave amplitudes ranged from 87.3  $\mu$ V to 180.3  $\mu$ V (average, 119.3  $\pm$  36.6  $\mu$ V) before and from 100.7  $\mu$ V to 195.8  $\mu$ V (average, 131.3  $\pm$  53.7  $\mu$ V; *P* = 0.444) after the vasohibin-1 injection. The b-wave amplitudes ranged from 219.6  $\mu$ V to 340.6  $\mu$ V (average 250.6  $\pm$  54.7  $\mu$ V) before and from 240.8  $\mu$ V to 345.2  $\mu$ V (average 274.4  $\pm$  82.0  $\mu$ V, *P* = 0.801) after the vasohibin-1 injection.

### *Effect of Different Concentrations of Vasohibin-1*

After the laser photocoagulation, we injected vehicle or 0.01, 0.1, or 1  $\mu$ g of vasohibin-1/50  $\mu$ L of vehicle in 3 eyes of each dosage for a total of 12 eyes (Table 1). From the results of safety evaluations, we selected the maximum amount of vasohibin-1 as 1  $\mu$ g of vasohibin-1/50  $\mu$ L of vehicle. Representative results of FA at 1, 2, and 4 weeks after the laser application for each dose of vasohibin-1 are shown in Figure 1. Color fundus photographs and focal ERGs recorded at 4 weeks are also shown.

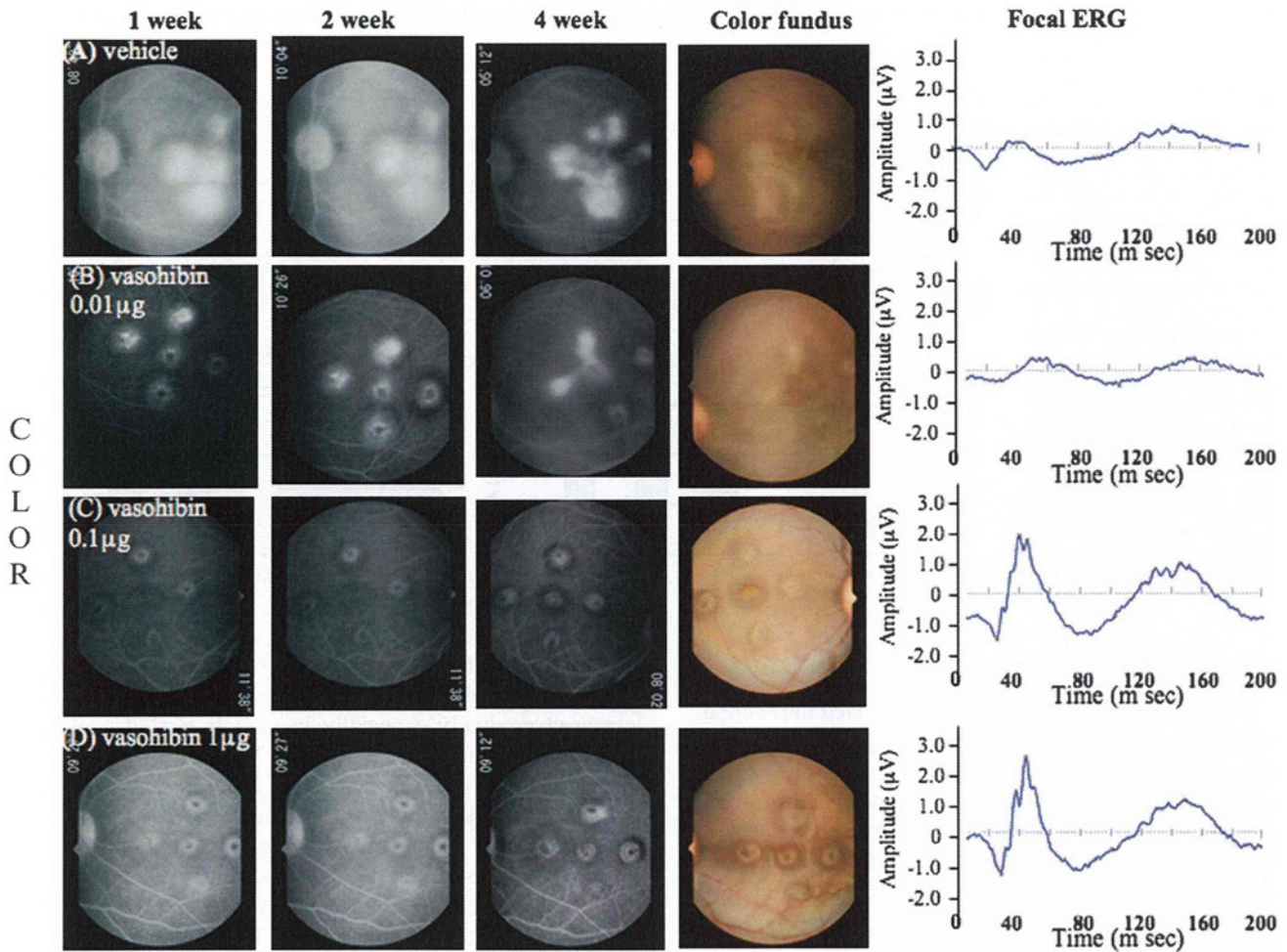


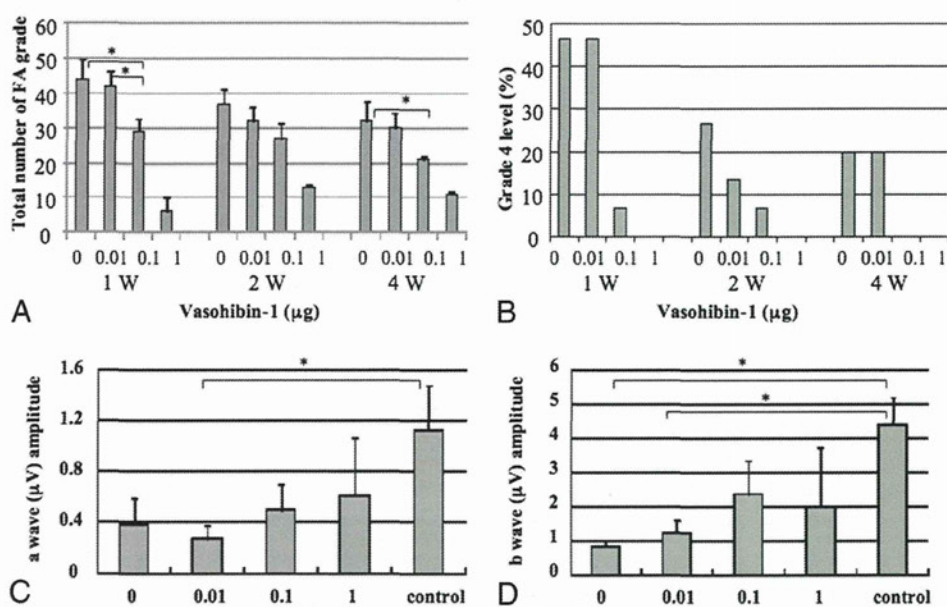
**Fig. 1.** Representative FAs, fundus photographs, and focal ERGs from 6 monkey eyes are shown. Vehicle or 0.01, 0.1, 1  $\mu\text{g}$  of vasohibin-1/50  $\mu\text{L}$  of vehicle was injected intravitreally, and representative results at 1, 2, and 4 weeks after laser treatment are shown (see quantitative values in Figure 2, A–D). The FA images are those at around 10 minutes after the fluorescein injection. Color fundus photographs were taken 4 weeks after the laser application. Focal ERGs recorded 4 weeks after the laser photocoagulation are shown in the right column for each eye.

The CNV activity was scored using the FA grading system<sup>22</sup> for all five laser spots in each eye. The FA score for each spot was summed and compared with each other (Figure 2A). Our findings showed that there was significantly less leakage after 0.1  $\mu\text{g}$  of vasohibin-1 than that for vehicle ( $P = 0.016$ ) and for 0.01  $\mu\text{g}$  ( $P = 0.035$ ) of vasohibin-1 at 1 week. Significantly less leakage after 0.1  $\mu\text{g}$  of vasohibin-1 than that of vehicle was also observed at 4 weeks ( $P = 0.0307$ ). Because 1  $\mu\text{g}$  of vasohibin-1 showed mild inflammation in 1 eye, we did not analyze the CNV in these eyes. The percentage of eyes with FA scores of 4 is also listed in Figure 2B. Our results showed that 45% of vehicle-treated eyes had Grade 4 leakage, and it was 45% in 0.01  $\mu\text{g}$  of vasohibin-1-treated eyes, 7% with 0.1  $\mu\text{g}$  of vasohibin-1-treated eyes, and

none in the 1- $\mu\text{g}$  vasohibin-1-treated eyes (only 2 eyes) at 1 week. Similarly, the percentage of eyes with Grade 4 leakage was 27%, 13%, 7%, and 0% at 2 weeks and 20%, 20%, 0% and 0% at 4 weeks after the vasohibin-1 injection (Figure 2B).

The amplitudes of the a-waves of the focal ERGs after 0.01  $\mu\text{g}$  of vasohibin-1 were significantly smaller than those of the controls ( $P = 0.041$ ) (Figure 2C). The amplitudes of the b-waves of the focal ERG b amplitudes in the vehicle-injected eyes ( $P = 0.0085$ ) and in the 0.01- $\mu\text{g}$  vasohibin-1-injected eye ( $P = 0.0184$ ) were significantly smaller than those of the controls (Figure 2D). The results of inflammation, FA leakage, and ERG amplitudes led us to select 0.1  $\mu\text{g}$  of vasohibin-1 as the optimal concentration for intravitreal injection to reduce the laser-induced CNV in our monkeys.

**Fig. 2.** Fluorescein angiographic scores for each of the 5 laser spots in each eye are plotted for each group, and the amplitudes of the a- and b-waves of the focal ERGs. **A.** Fluorescein angiographic scores for each of the five laser spots in each eye are plotted for each group. Statistically significant differences are shown as asterisks. **B.** Distribution of Grade 4 FA scores for each group is shown. **C** and **D.** Average amplitude of the a-waves (C) and b-waves (D) of the focal ERG recorded 4 weeks after intravitreal vasohibin-1. Vehicle (0) or 0.01, 0.10, or 1.00  $\mu\text{g}$  of vasohibin-1 was injected in control eyes or eyes after the laser burns. Untreated controls show the effects before laser treatment. The averages  $\pm$  standard deviations of the amplitudes of the a- and b-waves are plotted on the ordinate.



*Effects of Repeated Injections of Vasohibin-1*

Next, we examined the effects of repeated intravitreal injections of 0.1  $\mu\text{g}$  of vasohibin-1/50  $\mu\text{L}$  of vehicle in the right eyes on 0, 4, and 7 days after the laser application while the fellow eyes received an injection of the vehicle on the same days. We studied three eyes in each group. Representative fundus photographs, FAs, and OCT images after vehicle alone are shown in Figure 3 (A and B) and after 0.1  $\mu\text{g}$  of vasohibin-1/50  $\mu\text{L}$  of vehicle in Figure 3 (C and D). The FA scores were significantly lower in the vasohibin-1-injected eyes than in the vehicle-injected eyes at 4 weeks ( $P = 0.009$ ; Figures 3 and 4A). At 1 week and 2 weeks after the vasohibin-1 injections, the FA scores were not significantly different ( $P = 0.07$ ). The percentage of eyes scored as Grade 4 was 13.3% at 1 week, 26.7% at 2 weeks, and 26.7% at 4 weeks in the vehicle-treated eyes, whereas no Grade 4 eyes were observed in the 0.1  $\mu\text{g}$  of vasohibin-1/50  $\mu\text{L}$  of vehicle-treated eyes at any time (Figure 4B).

Although statistical significance was not observed in the a-wave amplitude of the focal ERGs, statistically significant larger b-wave amplitudes were observed in the vasohibin-1-treated eyes than that of vehicle ( $P = 0.039$ ) (Figure 4, C and D).

Optical coherence tomography examinations showed that the retinal pigment epithelium and Bruch membrane were disrupted in the laser-treated eyes at 1 week and 2 weeks after the laser application (Figure 3, B and D) as was found in histologic preparations.<sup>22</sup> At 4 weeks, an retinal pigment epithelium-like membrane appeared over the CNV lesion (Figure 3, B and D).

This line was shown to be cytokeratin positive. The OCT images showed that the size of the CNV increased gradually especially in vehicle-treated eyes as was seen in the FA images.

Optical coherence tomography also showed that the macular thickness (Figure 4E) and volume (Figure 4F) of the CNV lesions after 0.1  $\mu\text{g}$  of vasohibin-1/50  $\mu\text{L}$  of treated eyes was  $\sim 30\%$  less than the vehicle-treated eyes in the central 1 mm. When we examined the volume of the central 6 mm, no difference was observed between the vasohibin-1-treated and vehicle-treated eyes.

*Histology and Immunostaining of Choroidal Neovascularization*

Histopathologic analyses showed that the retina and choroid surrounding the CNV had normal architecture in both the vehicle and vasohibin-1-treated eyes as reported.<sup>26</sup> The vehicle-treated eyes after the laser application showed a disruption of the Bruch membrane and retinal pigment epithelium complex, and the eyes had different degrees of fibrous tissues and vessels (Figure 5, C and E). Eyes treated with vasohibin-1 tended to have smaller CNV than that of vehicle-treated eyes.

Cytokeratin labeling demonstrated that retinal pigment epithelial cells from the edges of the wound had proliferated and covered the laser wound to different degrees. Although a disruption of the cytokeratin labeling was present in the vehicle-treated eyes (Figure 5, D and F), we could not find any significant difference from that of the vasohibin-1-injected eyes. Different

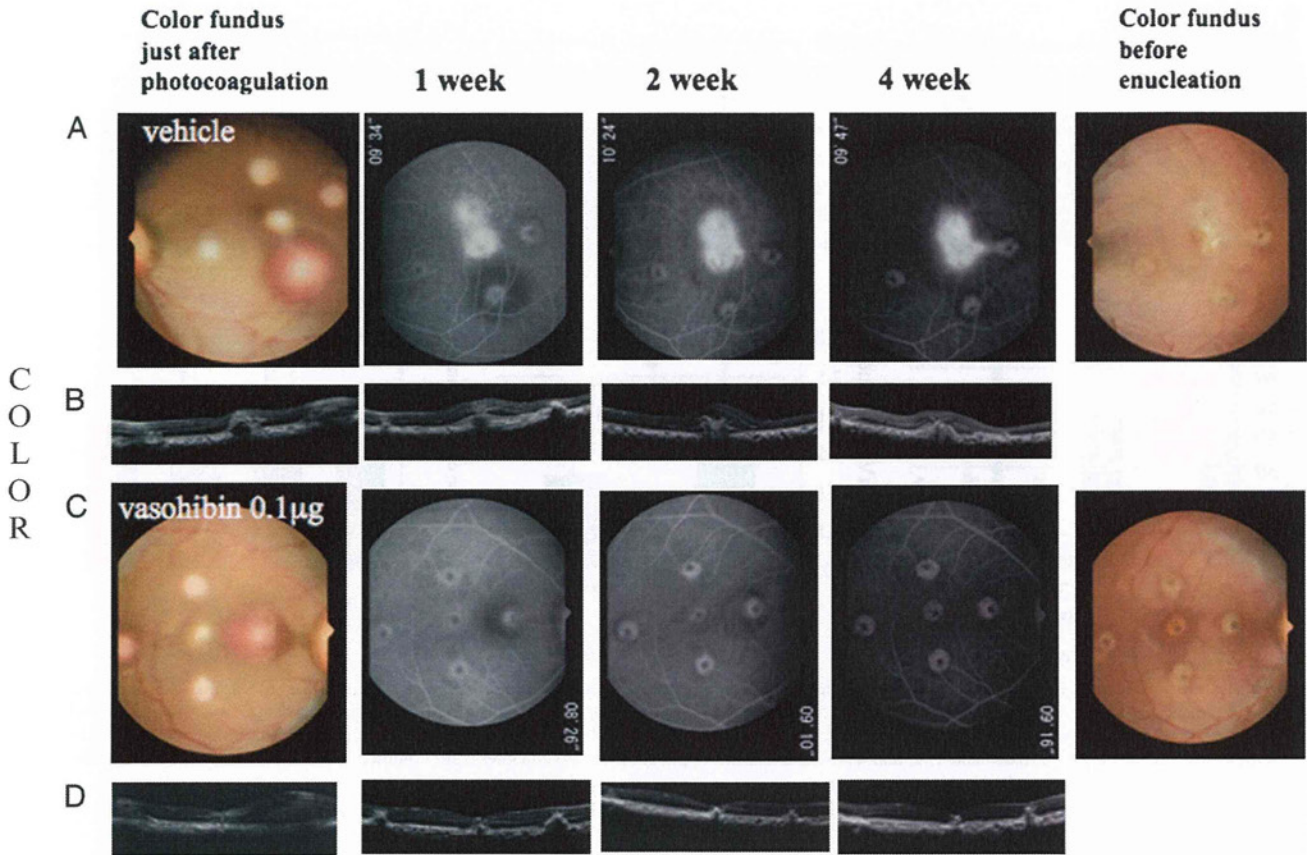


**Fig. 3.** Fluorescein angiograms, ocular coherence tomographic images, color fundus photographs, and focal ERGs are shown. Vasohibin-1 ( $0.1 \mu\text{g}/50 \mu\text{L}$ ) was injected into the vitreous of the right eyes 3 times on 0, 4, and 7 days after laser application, and the same amount of vehicle was injected into left eyes on the same days. Photographs show the fundus just after the laser application and the day of enucleation. Fluorescein angiograms recorded 1, 2, and 4 weeks after laser application. Photographs of the right (A) and left (C) eyes are shown. The results of OCT on the indicated days are shown in the same vertical columns for the indicated day (B) and (D).

numbers of macrophage-like cells were also observed in the neural retina.<sup>21</sup>

In immunostained eyes, vasohibin-1 positivity was found mainly in the CNV especially on the ECs in the CNV (Figure 5B). The regions surrounding the CNV showed little vasohibin-1-positive staining. Some monkeys showed no vasohibin-1 expression by immunohistochemistry even in the CNV at 28 day after laser application. Positive staining for vasohibin-1 appeared to be greater in the more active CNVs (Figure 5A), and it was more obvious in nontreated monkey eyes, although we could not determine whether the staining was significantly greater because only 3 monkey eyes were studied.

#### *Vascular Endothelial Growth Factor in Aqueous During Experiments*

The level of VEGF was determined by enzyme-linked immunosorbent assay. The average VEGF level in the aqueous in the vasohibin-1-injected

eyes was  $15.3 \text{ pg/mL}$ , and it was  $20.6 \text{ pg/mL}$  in the vehicle-treated eyes at 4 days after laser application. The average VEGF level in the vasohibin-1- and vehicle-treated eyes were  $7.0 \text{ pg/mL}$  and  $8.9 \text{ pg/mL}$ , respectively, at 4 weeks after laser application (Figure 6). For both times, the differences were not significant.

#### **Discussion**

Our results demonstrated that when  $10 \mu\text{g}$  or  $100 \mu\text{g}$  of vasohibin-1 was injected intravitreally into nontreated normal monkey eyes, a mild anterior chamber inflammation developed. No signs of inflammation or any adverse effects were found when  $<1 \mu\text{g}$  of vasohibin-1 was injected into nonlaser treated eyes, although we used only 1 eye for each dose. However when  $1 \mu\text{g}$  of vasohibin-1 was injected into laser-treated eyes, a mild inflammation developed in 1 of the 3 eyes. Inflammation has also been reported in monkey

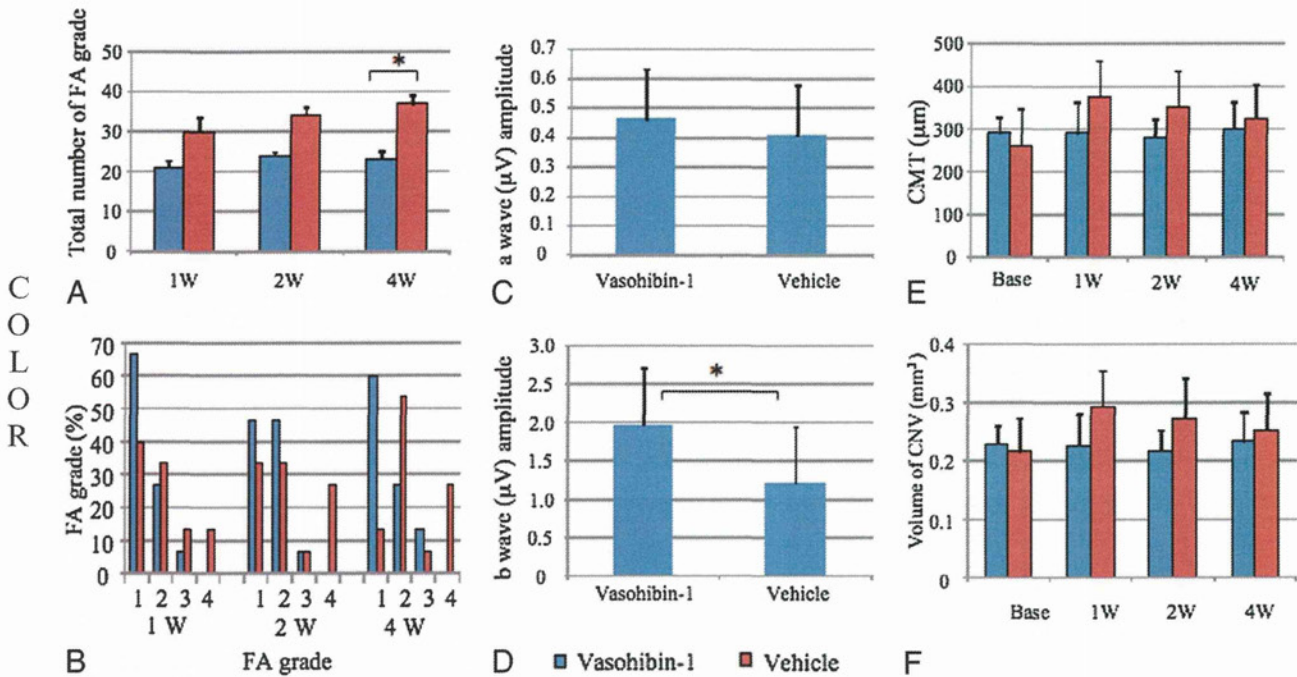


**Fig. 4.** Results of FA, focal ERG, and OCT are shown. **A.** Significantly less FA leakage was observed after 0.1 µg/50 µL of vasohibin-1 than after vehicle treatment at 4 weeks. **B.** Distribution of Grade 4 FA eyes for each group. **C** and **D.** Average amplitudes of the a-waves (**C**) and b-waves (**D**) of the focal ERGs. **E** and **F.** Average central macular thickness (CMT) and the central 3.4 mm and volume of area of either vasohibin-1-treated (blue) or vehicle-treated (red) eyes before (base) and 1, 2, and 4 weeks after laser application. Lower thickness and volumes were observed in the vasohibin-1-treated monkeys. Data are the standard deviations.

eyes after intravitreal injections of fragments of mouse and human chimera antibodies against VEGF.<sup>22,27</sup>

Fluorescein angiography examination after vasohibin-1 injection in laser-treated eyes showed significantly lower FA scores in eyes that received 0.1 µg and 1 µg of vasohibin-1 than the vehicle-injected eyes, although the number of eyes may have affected the statistics. Fluorescein leakage from the laser spots close to the macula was greater than that of the other laser spots. These results are compatible with the results of Shen et al,<sup>28</sup> who also found that the laser spot was larger and the leakage was greater for lesions closer to the macula. We also found that fluorescein leakage was different among monkeys, even though we applied the same amount of vasohibin-1.<sup>22</sup> This variability may be because the body weight ranged from 4.1 kg to 10.1 kg and age from 4 years to 6 years among the monkeys.

After we injected 0.1 µg of vasohibin-1 3 times in the right eyes and vehicle into the left eyes of 3 monkeys, we found significantly less fluorescein leakage in the vasohibin-1-treated right eyes than in the vehicle-treated eyes. The results of focal ERGs and OCT were well correlated with the results of FA findings, although the quantitative values were not significantly different.

Taken together, these results showed that intravitreal vasohibin-1 is able to reduce the activity of the laser-induced CNV in monkeys. With 3 injections of 0.1 µg of vasohibin-1, the results were not so different from that of only 1 injection at 4 days after the laser application. This may indicate that there may be an optimum time for the vasohibin-1 to affect the course of the laser-induced CNV. Alternatively, the results may be related to the half-life of vasohibin-1.

We found that vasohibin-1 was expressed on ECs especially those in the CNV lesions. Careful examinations showed that vasohibin-1 expression was limited to the CNV lesion and may not show extensive expression in other regions under normal physiologic conditions. Although we have not followed the expression of vasohibin-1 during the course of CNV development in monkeys, vasohibin-1 expression may be enhanced in the new vessels as was reported.<sup>29</sup> The vasohibin-1 expression appeared stronger in non-treated monkey eyes, although this could not be quantified. Vasohibin-1 has been reported to be present on the ECs only in the stroma of tumors and not in the noncancerous regions of the tissue in surgically resected tissues of the same patient.<sup>29</sup> These findings suggest that vasohibin-1 may be expressed mainly in the new vessels as it was in our laser-induced CNVs.

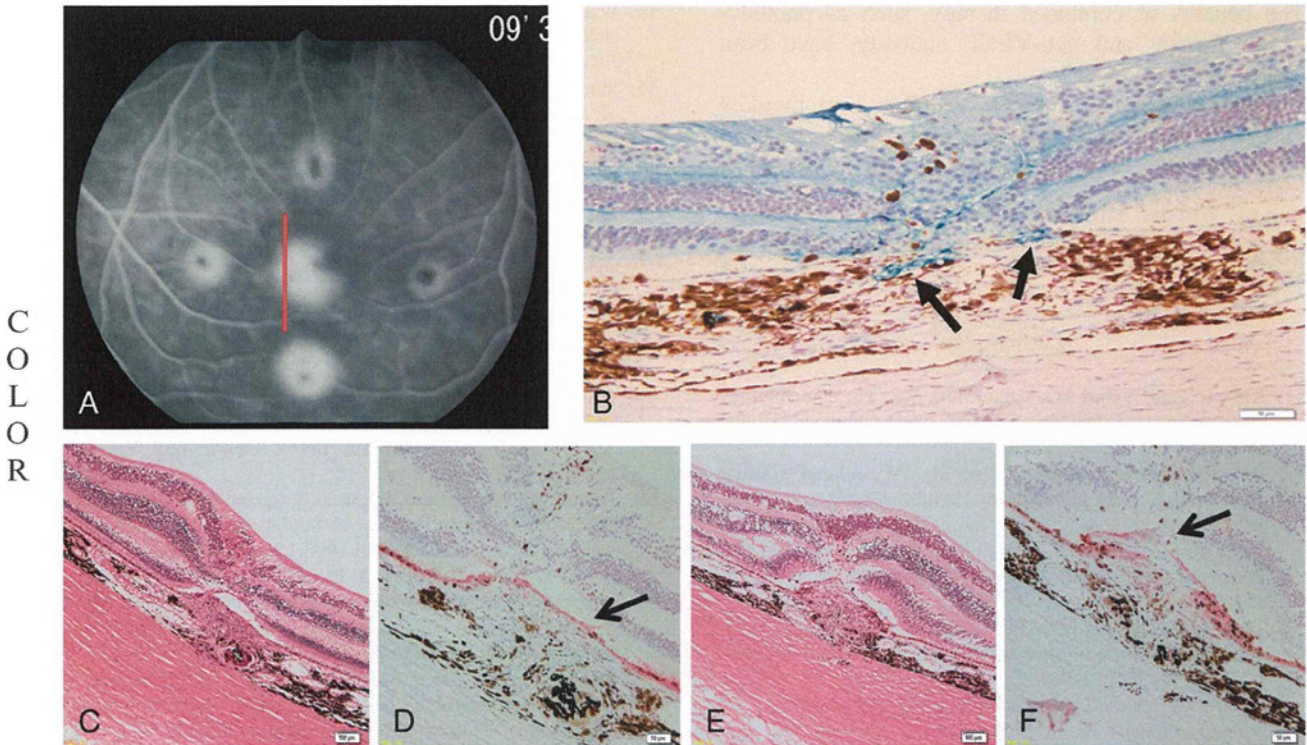


**Fig. 5.** Fluorescein angiograms 4 weeks after laser application or vehicle injection are shown. **A.** Immunohistochemistry for vasohibin-1 (**B**), the same eye as shown in (**A**) at the red line, is shown. Arrows indicate vasohibin-1 labeling. Vasohibin-1 expression is concentrated on the vessels around the CNV (arrows), but markedly less than in the CNV. Vasohibin-1 expression was observed at active CNV (red line in **A**). The subretinal space is an artifact of histologic processing. Cytokeratin labeling is also shown with vasohibin-treated eye (**D**) and vehicle-treated eye (**F**). Arrows show labeling of cyokeratin. Bar = 50  $\mu$ m. **C** and **E.** Hematoxylin and eosin staining of vasohibin-1-treated and vehicle-treated eyes, respectively, are shown. Bar = 100  $\mu$ m. Cytokeratin labeling shows that retinal pigment epithelium covers CNV in the vasohibin-1-treated eyes (**D**), and a disruption of cyokeratin labeling is observed in vehicle-treated eye (**F**).

Hosaka et al<sup>29</sup> reported that exogenous vasohibin-1 blocked angiogenesis and maturation of not only the cancerous tissue but also the surrounding vessels and, thus, enhanced the antitumor effects of

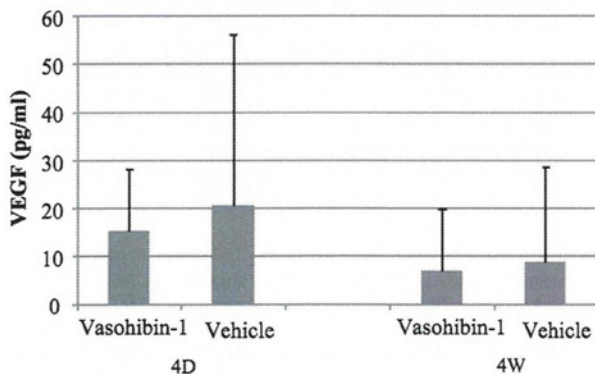


**Fig. 6.** Concentration of VEGF in aqueous in laser-treated monkey eyes 4 days and 4 weeks after laser application is shown. Vertical axis shows VEGF concentration in picograms per milliliter, and horizontal axis is the day of examination. Vascular endothelial growth factor in vasohibin-1-treated eyes (blue boxes) and vehicle-treated eyes (red boxes) show no significant difference at any times.

vasohibin-1. Intravitreal injection of vasohibin-1 may also suppress angiogenesis in CNVs by the same mechanism.

The amount of VEGF in the aqueous in the vasohibin-1-treated eyes did not differ from that in vehicle-treated eyes. Thus, Zhou et al<sup>30</sup> reported that external vasohibin-1 had no effect on the level of VEGF when they used adenovirus encoding human vasohibin-1 on mouse corneal neovascularization induced by alkali burn. They also reported that vasohibin-1 may downregulate the VEGF receptor 2 (VEGFR2). Shen et al<sup>16</sup> also reported a downregulation of VEGFR2 by vasohibin-1 during mouse ischemic retinopathy. Our previous studies have also shown a downregulation of VEGFR2 by external vasohibin-1 in laser-induced mouse CNVs.<sup>19</sup> Thus, vasohibin-1 may reduce the activity of a CNV by partially downregulating VEGFR2 in the eyes. If this is correct, vasohibin-1 may not affect the favorable aspects of VEGF such as its neuroprotective effect,<sup>31</sup> especially if VEGF works through VEGFR1 rather than VEGFR2. Vasohibin-1 also can be used with anti-VEGF antibody for CNV therapy.



The benefits of combined therapy, such as photodynamic therapy and anti-VEGF antibody, have been discussed.<sup>27</sup>

In conclusion, intravitreal vasohibin-1 in monkey eyes is safe and can reduce the activity of laser-induced CNVs and thus preserve the function of the macula.

**Key words:** choroidal neovascularization, laser-induced, monkey, vascular endothelial growth factor, vasohibin-1.

### References

- Klein R, Peto T, Bird AC, Vannewkirk MR. The epidemiology of age-related macular degeneration. *Am J Ophthalmol* 2004; 137:486–495.
- Bressler NM, Bressler SB, Fine SL. Age-related macular degeneration. *Surv Ophthalmol* 1998;32:375–413.
- Argon laser photocoagulation for neovascular maculopathy. Three-year results from randomized clinical trials Macular Photocoagulation Study Group. *Arch Ophthalmol* 1986;104: 694–701.
- Thomas MA, Grand MG, Williams DF, et al. Surgical management of subfoveal choroidal neovascularization. *Ophthalmology* 1992;99:952–968.
- Eckardt C, Eckardt U, Conrad HG. Macular rotation with and without counter-rotation of the globe in patients with age-related macular degeneration. *Graefes Arch Clin Exp Ophthalmol* 1999;237:313–325.
- Reichel E, Berrocal AM, Ip M, et al. Transpupillary thermotherapy of occult subfoveal choroidal neovascularization in patients with age-related macular degeneration. *Ophthalmology* 1999; 106:1908–1914.
- Photodynamic therapy of subfoveal choroidal neovascularization in age-related macular degeneration with verteporfin: one year results of 2 randomized clinical trials-TAP report Treatment of Age-related Macular Degeneration with Photodynamic Therapy (TAP). Study Group. *Arch Ophthalmol* 1999;117:1329–1345.
- Grisanti S, Tatar O. The role of vascular endothelial growth factor and other endogenous interplayers in age-related macular degeneration. *Prog Retin Eye Res* 2008;27:372–390.
- Miller JW, Adamis AP, Shima DT, et al. Vascular endothelial growth factor/vascular permeability factor is temporally and spatially correlated with ocular angiogenesis in a primate model. *Am J Pathol* 1994;145:574–584.
- Krzystolik MG, Afshari MA, Adamis AP, et al. Prevention of experimental choroidal neovascularization with intravitreal anti-vascular endothelial growth factor antibody fragment. *Arch Ophthalmol* 2002;120:338–346.
- Rosenfeld PJ, Brown DM, Heier JS, et al. Ranibizumab for neovascular age-related macular degeneration. *N Engl J Med* 2006;355:1419–1431.
- Pilli S, Kotsolis A, Spaide RF, et al. Endophthalmitis associated with intravitreal anti-vascular endothelial growth factor therapy injections in an office setting. *Am J Ophthalmol* 2008;145:879–882.
- Lux A, Llacer H, Heussen FMA, Jousseaume AM. Non-responders to bevacizumab (Avastin) therapy of choroidal neovascular lesions. *Am J Ophthalmol* 2007;91:1318–1322.
- Watanabe K, Hasegawa Y, Yamashita H, et al. Vasohibin as an endothelium-derived negative feedback regulator of angiogenesis. *J Clin Invest* 2004;114:898–907.
- Shimizu K, Watanabe K, Yamashita H, et al. Gene regulation of a novel angiogenesis inhibitor, vasohibin, in endothelial cells. *Biochem Biophys Res Commun* 2005;327:700–706.
- Shen J, Yang X, Xiao WH, et al. Vasohibin is up-regulated by VEGF in the retina and suppresses VEGF receptor 2 and retinal neovascularization. *FASEB J* 2006;20:723–725.
- Sato H, Abe T, Wakusawa R, et al. Vitreous levels of vasohibin-1 and vascular endothelial growth factor in patients with proliferative diabetic retinopathy. *Diabetologia* 2009;52:359–361.
- Wakusawa R, Abe T, Sato H, et al. Expression of vasohibin, an antiangiogenic factor, in human choroidal neovascular membranes. *Am J Ophthalmol* 2008;146:235–243.
- Wakusawa R, Abe T, Sato H, et al. Suppression of choroidal neovascularization by vasohibin-1, vascular endothelium-derived angiogenic inhibitor. *Invest Ophthalmol Vis Sci* 2011;52:3272–3280.
- Tobe T, Ortega S, Luna JD, et al. Targeted disruption of the FGF2 gene does not prevent choroidal neovascularization in a murine model. *Am J Pathol* 1998;153:1641–1646.
- Heishi T, Hosaka T, Suzuki Y, et al. Endogenous angiogenesis inhibitor vasohibin1 exhibits broad-spectrum antilymphangiogenic activity and suppresses lymph node metastasis. *Am J Pathol* 2010;176:1950–1958.
- Krzystolik MG, Afshari MA, Adamis AP, et al. Prevention of experimental choroidal neovascularization with intravitreal anti-vascular endothelial growth factor antibody fragment. *Arch Ophthalmol* 2002;120:338–346.
- Miyake Y, Yanagida K, Yagasaki K, et al. Subjective scotometry and recording of local electroretinogram and visual evoked response. System with television monitor of the fundus. *Jpn J Ophthalmol* 1981;25:439–448.
- Kondo M, Ueno S, Piao CH, et al. Comparison of focal macular cone ERGs in complete-type congenital stationary night blindness and APB-treated monkeys. *Vision Res* 2008;48: 273–280.
- Hogan MJ, Kimura SJ, Thygeson P. Signs and symptoms of uveitis. I. Anterior uveitis. *Am J Ophthalmol* 1959;47:155–170.
- Zhang M, Zhang J, Yan M, et al. Recombinant anti-vascular endothelial growth factor fusion protein efficiently suppresses choroidal neovascularization in monkeys. *Mol Vision* 2008;14:37–49.
- Husain D, Kim I, Gauthier D, et al. Safety and efficacy of intravitreal injection of ranibizumab in combination with verteporfin PDT on experimental choroidal neovascularization in the monkey. *Arch Ophthalmol* 2005;123:509–516.
- Shen WY, Lee SY, Yeo I, et al. Predilection of the macular region to high incidence of choroidal neovascularization after intense laser photocoagulation in the monkey. *Arch Ophthalmol* 2004;122:353–360.
- Hosaka T, Kimura H, Heishi T, et al. Vasohibin-1 expression in endothelium of tumor blood vessels regulates angiogenesis. *Am J Pathol* 2009;175:430–439.
- Zhou SY, Xie ZL, Xiao O, et al. Inhibition of mouse alkali burn induced-corneal neovascularization by recombinant adenovirus human vasohibin-1. *Mol Vision* 2010;16:1389–1398.
- Alon T, Hemo I, Itin A, et al. Vascular endothelial growth factor acts as a survival factor for newly formed retinal vessels and has implications for retinopathy of prematurity. *Nat Med* 1995;1:1024–1028.

## Chapter 40

# Vasohibin-1 and Retinal Pigment Epithelium

Yumi Ishikawa, Nobuhiro Nagai, Hideyuki Onami, Norihiro Kumasaka, Ryosuke Wakusawa, Hikaru Sonoda, Yasufumi Sato, and Toshiaki Abe

**Keywords** Vasohibin • VEGF • Retinal pigment epithelium • Hypoxia • Cell dynamics • Cobalt chloride

### 40.1 Introduction

Choroidal neovascularization (CNV) leads to subretinal hemorrhages, exudative lesions, serous retinal detachment, and disciform scars in patients with age-related macular degeneration (AMD) (Bressler et al. 1998). Vascular endothelial growth factor (VEGF), a pro-angiogenic factor, plays a major role in the development of CNV (Spilsbury et al. 2000). Recently, anti-VEGF treatment for patients with AMD has developed and reported good results (Krzystolik et al. 2002; Rosenfeld et al. 2006). However, there are many problems, such as repeated intravitreal injections, side effects (Pilli et al. 2008), suppression of the important physiological VEGF function (Alon et al. 1995), and further not all patients respond well to this therapy (Lux et al. 2007). Vasohibin-1 is a VEGF-inducible gene in human cultured endothelial cells (ECs) with antiangiogenic properties (Watanabe et al. 2004; Sonoda et al. 2006). Vasohibin-1 is induced by several pro-angiogenic factors such as VEGF and

---

Y. Ishikawa • N. Nagai • H. Onami • N. Kumasaka • R. Wakusawa • T. Abe (✉)  
Division of Clinical Cell Therapy, United Center for Advanced Research and Translational  
Medicine (ART), Tohoku University Graduate School of Medicine, 1-1 Seiryomachi Aobaku  
Sendai, Miyagi, Japan  
e-mail: toshi@oph.med.tohoku.ac.jp

H. Sonoda  
Discovery Research Laboratories, Shionogi and Co. Ltd. Osaka, Japan

Y. Sato  
Department of Vascular Biology, Institute of Development, Aging, and Cancer,  
Tohoku University Graduate School of Medicine, Miyagi, Japan

basic fibroblast growth factor (bFGF) (Watanabe et al. 2004). We showed that the vasohibin-1/VEGF ratio might play a role for clinical significance of CNV in patients with AMD using surgically excised CNV membranes (Wakusawa et al. 2008). The membranes included not only ECs but also retinal pigment epithelium (RPE). In this report, we examined the effects of vasohibin-1 on RPE.

## 40.2 Methods

### 40.2.1 RPE Preparation

We used commercially available rat RPE cell line, RPE-J. RPE-J was cultured in DMEM/F-12 medium with 4% fetal bovine serum (FBS; Sigma, St. Louis MO) with 5% CO<sub>2</sub> supply at 33°C. Human vasohibin-1 cDNA with antineomycin gene vector was transduced into RPE-J as we previously reported (Abe et al. 2008). Cells that were stably introduced the vector were selected by antibiotics. We selected 18 clones on both vasohibin-1 cDNA and only vector-transduced RPE-Js. Cobalt chloride (100–300 μM) and low glucose (0–100 μM) and oxygen supply (2%) were used for hypoxic stress. Vasohibin-1 was supplied from Shionogi and Co. Ltd, Osaka, Japan and VEGF and other chemicals were purchased from Wako (Tokyo Japan).

### 40.2.2 Real-Time RPE Impedance Analysis and MTS Assay

Dynamic cellular biology of the cultured RPE was monitored using Real-Time Cell Analyzer (RTCA), xCELLigence System (Roche Applied Science, Mannheim, Germany). The system evaluates cellular events in real time measuring electrical impedance at an electrode/solution interface at the bottom of cell culture plates. The system provides cell number, viability, morphology, and adhesion described as Cell Index (CI). RPE proliferation was also evaluated by 3-(4, 5-dimethylthiazol-2-yl)-5-(3-carboxymethoxyphenyl)-2-(4-sulfophenyl)-2H-tetrazolium, inner salt (MTS) assay, and counting cell number for each condition.

### 40.2.3 Extraction of mRNA, cDNA Generation, Reverse-Transcriptase, and Real-Time Polymerase Chain Reaction (RT-PCR)

mRNA was extracted and cDNAs were generated from the cells according to the manufacturer's instructions (Pharmacia Biotech Inc., Uppsala, Sweden). Semiquantitative real-time PCR was carried out by the primer sets described below (LightCycleST300:Roche, Basel, Swiss). The sequences were 5'-TCT GCT CTC

TTG GGT GCA AT-3' and 5'-TTC CGG TGA GAG GTC CGG TT-3' for VEGF, 5'-GAT TCC CAT ACC AAG TGT GCC-3' and 5'-ATG TGG CGG AAG TAG TTC CC-3' for vasohibin-1, and 5'-CATCACCATCTTCCAGGAGC-3' and 5'-CATGAGTCCTTCCACGATACC-3' for GAPDH. All data were normalized to the GAPDH expression level, thus giving the relative expression level.

#### **40.2.4 Western Blot Analysis for Vasohibin-1 and VEGF**

Cells were collected and used for western blotting analysis after sonication, as we reported previously (Abe et al. 2008). Cells were washed in ice-cold Dalbecco's phosphate buffered saline (DPBS) 3 times, and then immediately sonicated in lysis buffer. After blotting on Immune-Blot PVDF Membrane (BIO-RAD Laboratories, CA), it was incubated overnight in mouse antivasohibin-1 or anti-VEGF antibody (Santa Cruz) at 4°C and visualized using an enhanced chemiluminescence system (ECL Plus, GE Healthcare) according to the manufacturer's instructions.

### **40.3 Results**

#### **40.3.1 Vasohibin-1 Expression**

Vasohibin-1 expression in the RPE was confirmed by real-time PCR and western blot analysis. When we cultured the cells with cobalt chloride, a pseudo-hypoxic condition, or low oxygen (2%), 1% serum, and no glucose, gradual upregulation of VEGF gene was observed with 100- $\mu$ M cobalt chloride (Fig. 40.1a). Conversely, statistically significant low vasohibin-1 expression was observed with 100- $\mu$ M cobalt chloride at more than 12-h culture when compared to those of standard culture or less than 6-h culture (Fig. 40.1b). Western blot analysis showed that vasohibin-1 expression seemed to be downregulated at more than 36-h culture with 100- $\mu$ M cobalt chloride (Fig. 40.1c).

#### **40.3.2 RPE Dynamics and Proliferation by Vasohibin-1**

An RTCA was used to monitor dynamic changes in the properties of RPE cells during the culture. The parameter of CI shows cell viability, number, morphology, and adhesion to the bottom of the plates. When we cultured the cells under standard condition as described above, we found no difference of CI even though we added VEGF (Fig. 40.2a) and/or vasohibin-1 (Fig. 40.2b). When we added VEGF (0.2–10 nM) in the culture medium at 2% oxygen, 1% serum, and no glucose, we found that VEGF enhanced CI (Fig. 40.2c). Statistically significant difference was observed when we cultured the cells more than 15 h after treatments with 1 and 2-nM VEGF.

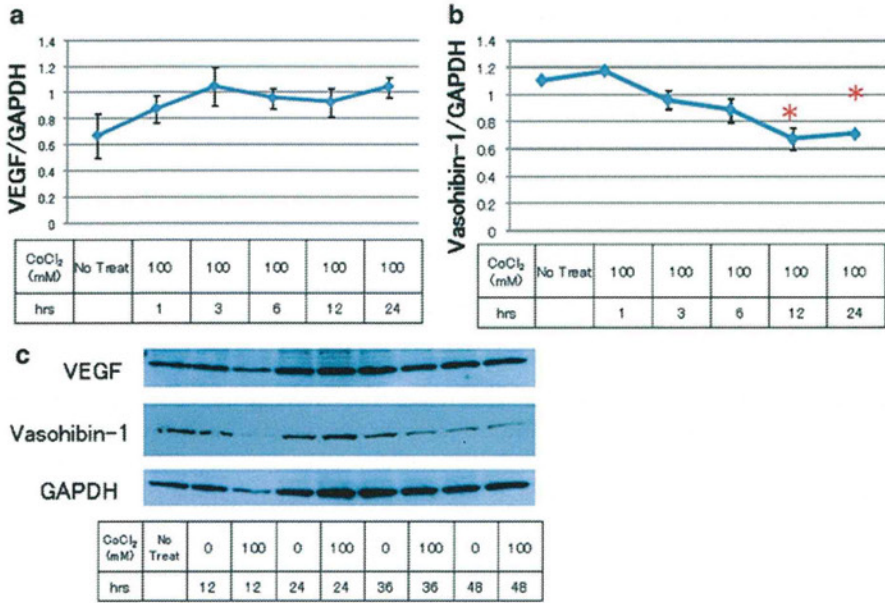


**Fig. 40.1** Real-time PCR of VEGF (a) and vasohibin-1 (b) genes is shown. VEGF gene was upregulated in RPE-J with cobalt chloride during successive culture whereas vasohibin-1 gene was suppressed. Western blot analysis (c) shows decreased vasohibin-1 expression at the condition

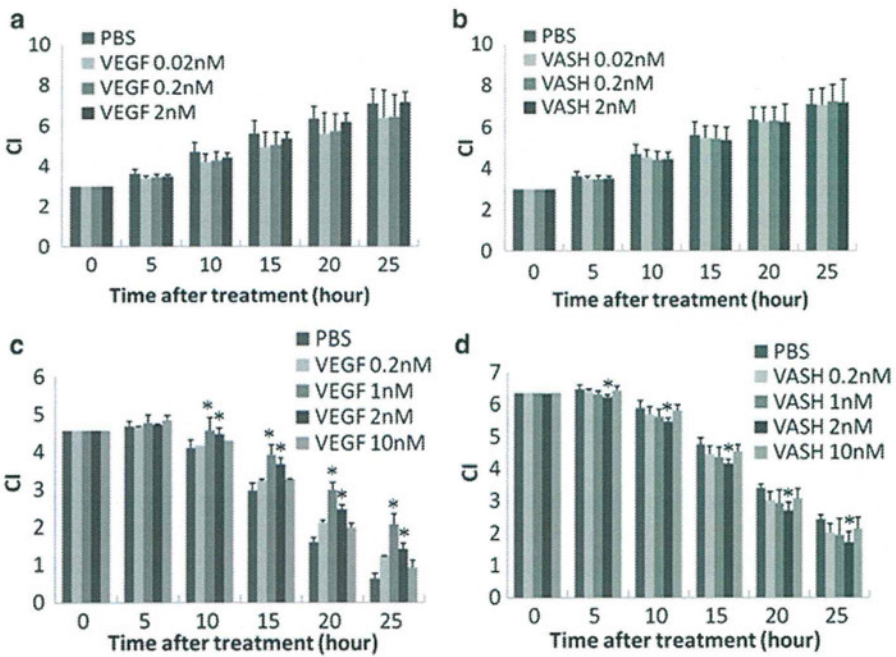


**Fig. 40.2** Cell Index of RTCA shows that VEGF enhanced CI at hypoxic condition (a), conversely vasohibin-1 reduced CI only at hypoxic condition (b). The results were not observed at normal condition

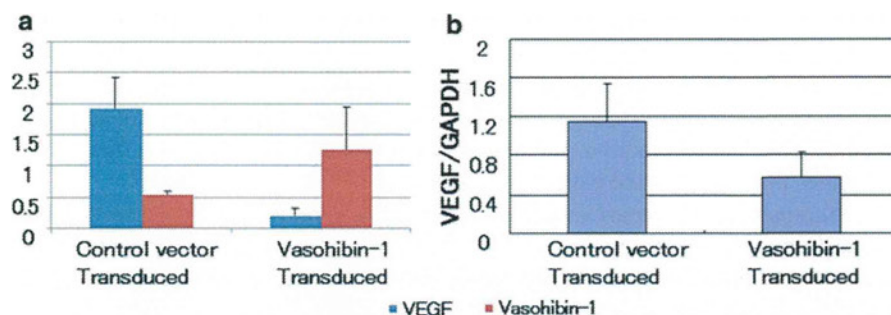


**Fig. 40.3** Human vasohibin-1 gene was transduced into RPE-J. We selected 18 clones on both vasohibin-1 gene transduced and only vector-transduced RPE-J. Statistically significant less VEGF gene expression was observed in vasohibin-1 gene-transduced cDNA when compared to that of vector-transduced cDNA (a). Western blot analysis also showed comparable results (b)

Conversely, when we applied vasohibin-1 (0.2–10 nM) in the culture medium at 2% oxygen, 1% serum, and no glucose, we found that vasohibin-1 showed lower CI (Fig. 40.2d). Statistically significant difference was observed at 2-nM vasohibin-1. Vasohibin-1 application also showed statistically significant small cell number either 300- $\mu$ M cobalt chloride or 2% oxygen, 1% serum, and no glucose. When we performed MTS assay, statistically significant less cell proliferation was also observed at these indicated conditions. When we examined the apoptotic cells, there was no significant difference. Human vasohibin-1 gene-transduced RPE-J showed statistically significant less VEGF expression when compared to those of vector-transduced cell by real-time PCR and western blot analysis (Fig. 40.3a, b).

#### 40.4 Discussion

Vasohibin-1 is an endogenous antiangiogenic agent that is induced by variable proangiogenic factors such as VEGF and bFGF. Vasohibin-1 was reported to inhibit the sprouting of new vessels and to support vascular maturation processes (Kimura et al. 2009). These antiangiogenic properties were detected after recombinant vasohibin-1 was used for corneal and retinal neovascularization (Watanabe et al. 2004). We have found that vasohibin-1 is expressed on ECs of choroidal and retinal vessels, human CNV membranes (Wakusawa et al. 2008), and proliferative membranes of diabetic retinopathy (Sato et al. 2009). In addition, we suggested that the vasohibin-1/VEGF ratio was related to the activity of the CNV (Wakusawa et al. 2008). RPE is known for secreting VEGF from its basal side to choriocapillaris direction and performs important function for the survival of the vascular ECs and nonvascular cells developmentally and also in adults (Alon et al. 1995). This mechanism also maintains low VEGF concentration at subretinal space (Peng et al. 2010). Because of this specific function, we examined the correlation of vasohibin-1 and VEGF on RPE. From the results of present study, vasohibin-1 was expressed in RPE and the

expression was suppressed under hypoxic condition in RPE-J. Vasohibin-1 was also suspected to inhibit VEGF function of rat RPE. Interestingly, these results were observed only at hypoxic conditions and not in standard culture condition. Together with the previous reports, these results may show that vasohibin-1 may not suppress physiological VEGF function. External vasohibin-1 may participate as one of the molecules that suppress the pathological CNV.

In summary, we examined vasohibin-1 expression in rat RPE and the effects under normal or hypoxic condition. Vasohibin-1 expression was suppressed under hypoxic conditions. External vasohibin-1 plays an important role on RPE, especially in hypoxic condition, and suppresses VEGF function on rat RPE.

**Acknowledgments** This study was supported in part by grants from Grants-in-Aid for Scientific Research 20592030, 21592214 from the Japan Society for the Promotion of Science, Chiyoda-ku, Tokyo, Japan and Suzuken Memorial Foundation.

## References

- Abe T, Wakusawa R, Seto H et al (2008) Topical doxycycline can induce expression of BDNF in transduced retinal pigment epithelial cells transplanted into the subretinal space. *Invest Ophthalmol Vis Sci* 49: 3631–3639
- Alon T, Hemo I, Itin A et al (1995) Vascular endothelial growth factor acts as a survival factor for newly formed retinal vessels and has implications for retinopathy of prematurity. *Nat Med* 1: 1024–1028
- Bressler NM, Bressler SB, Fine SL (1998) Age-related macular degeneration. *Surv Ophthalmol* 32: 375–413
- Kimura H, Miyashita H, Suzuki Y et al (2009) Distinctive localization and opposed roles of vasohibin-1 and vasohibin-2 in the regulation of angiogenesis. *Blood* 113: 4810–4818
- Krzystolik MG, Afshari MA, Adamis AP et al (2002) Prevention of experimental choroidal neovascularization with intravitreal anti-vascular endothelial growth factor antibody fragment. *Arch Ophthalmol* 120: 338–346
- Lux A, Llacer H, Heussen FMA et al (2007) Non-responders to bevacizumab (Avastin) therapy of choroidal neovascular lesions. *Am J Ophthalmol* 91: 1318–1322
- Peng S, Adelman RA, Rizzolo LJ (2010) Minimal effects of VEGF and anti-VEGF drugs on the permeability or selectivity of RPE tight junctions. *Invest Ophthalmol Vis Sci* 51: 3216–3225
- Pilli S, Kotsolis A, Spaide RF et al (2008) Endophthalmitis associated with intravitreal anti-vascular endothelial growth factor therapy injections in an office setting. *Am J Ophthalmol* 145: 879–882
- Rosenfeld PJ, Brown DM, Heier JS et al (2006) MARINA Study Group. Ranibizumab for neovascular age-related macular degeneration. *N Engl J Med* 355: 1419–1431
- Sato H, Abe T, Wakusawa R et al (2009) Vitreous levels of vasohibin-1 and vascular endothelial growth factor in patients with proliferative diabetic retinopathy. *Diabetologia* 52: 359–361
- Sonoda H, Ohta H, Watanabe K et al (2006) Multiple processing forms and their biological activities of a novel angiogenesis inhibitor vasohibin. *Biochem Biophys Res Commun* 342: 640–646
- Spilsbury K, Garrett KL, Shen WY et al (2000) Overexpression of vascular endothelial growth factor (VEGF) in the retinal pigment epithelium leads to the development of choroidal neovascularization. *Am J Pathol* 157: 135–144
- Wakusawa R, Abe T, Sato H et al (2008) Expression of vasohibin, an antiangiogenic factor, in human choroidal neovascular membranes. *Am J Ophthalmol* 146: 235–243
- Watanabe K, Hasegawa Y, Yamashita H et al (2004) Vasohibin as an endothelium-derived negative feedback regulator of angiogenesis. *J Clin Invest* 114: 898–907





厚生労働科学研究費補助金  
障害者対策総合研究事業

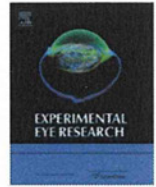
新規薬剤の生体内スクリーニングシステムの確立と  
網膜保護用デバイスの開発

平成24年度 総括・分担研究報告書

研究代表者 阿部 俊明

平成25 (2013) 年 5月

(2 / 2冊)



## Comparison of CCD-equipped laser speckle flowgraphy with hydrogen gas clearance method in the measurement of optic nerve head microcirculation in rabbits

Hiroaki Takahashi<sup>a</sup>, Tetsuya Sugiyama<sup>b,\*</sup>, Hideki Tokushige<sup>a</sup>, Takatoshi Maeno<sup>c</sup>, Toru Nakazawa<sup>d</sup>, Tsunehiko Ikeda<sup>b</sup>, Makoto Araie<sup>e</sup>

<sup>a</sup> Research Laboratory for Drug Development, Senju Pharmaceutical Co., Ltd., 1-5-4 Murotani, Nishi-ku, Kobe, Hyogo 651-2241, Japan

<sup>b</sup> Department of Ophthalmology, Osaka Medical College, 2-7 Daigaku-machi, Takatsuki, Osaka 569-8686, Japan

<sup>c</sup> Department of Ophthalmology, Toho University Sakura Medical Center, 564-1 Shimoshizu, Sakura, Chiba 285-8741, Japan

<sup>d</sup> Department of Ophthalmology, Tohoku University Graduate School of Medicine, 1-1 Seiryō-machi, Aoba-ku, Sendai, Miyagi 980-8574, Japan

<sup>e</sup> Kanto Central Hospital of The Mutual Aid Association of Public School Teachers, 6-25-1 Kamiyoga, Setagaya-ku, Tokyo 158-0098, Japan

### ARTICLE INFO

#### Article history:

Received 6 October 2012

Accepted in revised form 10 December 2012

Available online 19 December 2012

#### Keywords:

optic nerve head  
laser speckle flowgraphy  
mean blur rate  
hydrogen gas clearance method  
capillary blood flow  
rabbit

### ABSTRACT

The aim of this study was to verify the correlation between mean blur rate (MBR) obtained with CCD-equipped laser speckle flowgraphy (LSFG) and capillary blood flow (CBF) obtained by the hydrogen gas clearance method in rabbit optic nerve head (ONH). Using Japanese white rabbits under systemic anesthesia, a hydrogen electrode was inserted an area of the ONH free from superficial capillaries. MBR was measured with LSFG near the hydrogen electrode. CBF and MBR were measured in the range of 32.4–83.5 mL/min/100 g and 3.5–6.0, respectively. MBR and CBF were significantly correlated ( $r = 0.73$ ,  $P < 0.01$ ,  $n = 14$ ). After inhalation of carbon dioxide (CO<sub>2</sub>) or intravenous administration of endothelin-1 (ET-1), MBR and CBF were changed in the relative range of 0.74–1.27 and 0.76–1.35, respectively. The relative changes in MBR and CBF induced by CO<sub>2</sub> and ET-1 were also significantly correlated ( $r = 0.67$ ,  $P < 0.01$ ). The current results suggest that MBR may correlate with CBF and also change with CBF, as an index of blood flow in the ONH, linearly.

© 2012 Elsevier Ltd. All rights reserved.

### 1. Introduction

Abnormal blood flow regulation is widely recognized to contribute to the pathophysiology of ocular diseases such as glaucoma (Grieshaber et al., 2007; Moore et al., 2008; Pemp et al., 2009). Circulatory factors in the retrobulbar arteries may be associated with the progression of visual field defects in patients with normal-tension glaucoma (Yamazaki and Drance, 1997). Progressive structural changes in the optic nerve head (ONH) also have been related to abnormal ocular blood flow in glaucoma patients (Harris et al., 2008b). For example, Logan et al. (2004) found lower levels of retinal blood flow in abnormal segments of the ONH than in a corresponding normal segment in glaucoma patients. In addition, glaucoma patients with normal rim segments demonstrated lower

retinal blood flow than controls at each location sampled. However, the role played by blood flow and ischemia on the ONH and retina in glaucoma has not yet been clarified, in part because technical difficulties have limited the accurate measurement of ocular blood flow in relevant vascular beds (Caprioli and Coleman, 2010; Harris et al., 2008a).

The Association for Ocular Circulation (<http://www.obfra.org/>) has published consensus reports on ocular circulation measurement methods such as laser Doppler flowmetry (Riva et al., 2010), laser speckle flowgraphy (LSFG) (Sugiyama et al., 2010), retinal vessel analysis (Garhofer et al., 2010), and color Doppler imaging (Stalmans et al., 2011). Among them, LSFG is the only method available to measure tissue circulation non-invasively and provide a 2-dimensional map of ocular tissue circulation. Normalized blur (NB) was the value used previously in LSFG and represents an index of blood velocity (Tamaki et al., 1994, 1995). *In vitro*, NB demonstrated a good linear correlation with the mean velocity of blood cells flowing through a glass capillary tube (calculated from the blood flow rate generated by a calibrated peristaltic pump) (Nagahara et al., 1999) and with the speed of rotation of a ground-

Abbreviations: CBF, capillary blood flow; LSFG, laser speckle flowgraphy; MBR, mean blur rate; ONH, optic nerve head.

\* Corresponding author. Tel.: +81 72 683 1221; fax: +81 72 681 8195.

E-mail addresses: [tsugiyama@poh.osaka-med.ac.jp](mailto:tsugiyama@poh.osaka-med.ac.jp), [tsugiyama7@gmail.com](mailto:tsugiyama7@gmail.com) (T. Sugiyama).

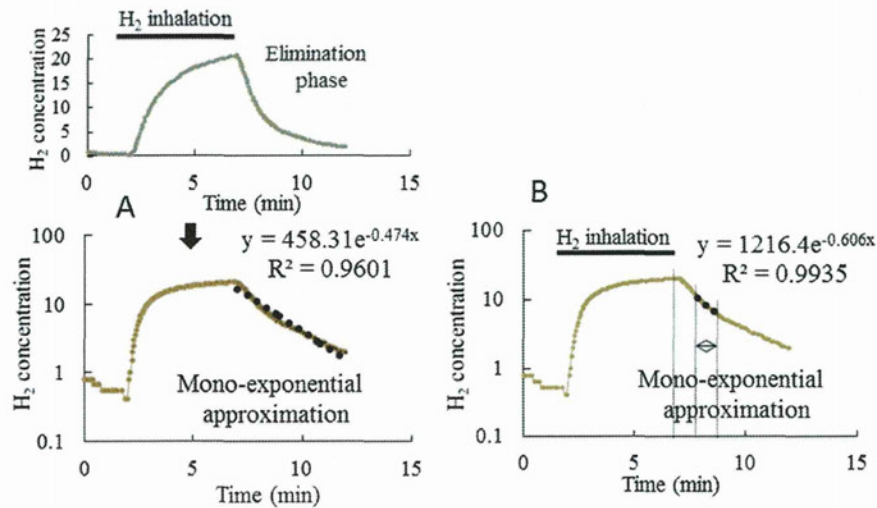


**Fig. 1.** An example of analyzing hydrogen clearance curve to obtain capillary blood flow (CBF) by the hydrogen gas clearance method. The hydrogen concentration was plotted into logarithm (A). The half-life ( $T_{1/2}$ ) at 1–2 min after stopping hydrogen inhalation was adopted for calculation because the linearity of hydrogen clearance in logarithm was the highest there (B). We then calculate CBF as  $69.3/T_{1/2}$  (ml/min/100 g).

glass disc (calculated from the velocity of diffusing particles, which are models of blood cells, on the glass) (Nagahara et al., 1999; Tamaki et al., 1994, 1995, ). *In vivo*, NB was well correlated with tissue blood flow rates determined using the microsphere method in the retina, choroid, or iris, as well as blood flow rates determined with the hydrogen gas clearance method in the ONH (Sugiyama et al., 1996; Takayama et al., 2003; Tamaki et al., 1994, 1995, 1996, 2003; Tomidokoro et al., 1998; Tomita et al., 1999).

In 2008, LSF<sub>G</sub>-NAVI™ was approved as a medical apparatus by the Pharmaceuticals and Medical Devices Agency in Japan. It has adopted a new index: mean blur rate (MBR), the relative velocity index of erythrocytes (Konishi et al., 2002; Watanabe et al., 2008). Recently, Aizawa et al. (2011) reported that MBR has high reproducibility in normal and glaucoma subjects. However, no reports to date have investigated whether MBR is correlated with blood flow rate in the ONH.

The hydrogen gas clearance technique provides multiple capillary blood flow (CBF) measurements quantitatively over long periods of time (Aukland et al., 1964; Csete et al., 2004; Srinivasan

et al., 2011). In the ophthalmic field, this technique has been applied to the ONH in rhesus monkeys (Ernest, 1976) and demonstrated high reproducibility in the measurement of CBF in rabbit ONH (Sugiyama et al., 1995). However, use of this technique is limited to laboratory research because it is highly invasive. The aim of the current study was to verify the correlation between MBR obtained by LSF<sub>G</sub> and CBF obtained by the hydrogen gas clearance method in the rabbit ONH.

## 2. Materials and methods

### 2.1. Animals

Eighteen male Japanese white rabbits weighing 2.5–3.3 kg were purchased from Kitayama Lab. (Nagano, Japan) for the current study. They were housed in an air-conditioned room at temperature of  $23 \pm 3$  °C and humidity of  $55 \pm 10\%$  with a 12-h light–dark cycle and provided with tap water *ad libitum* throughout the experimental period. All animal studies were performed in accordance with the ARVO statement for the use of animals in ophthalmic and vision research and with the approval of the Institutional Animal Care and Use Committee of Kobe Creative Center, Senju Pharmaceutical Co., Ltd.

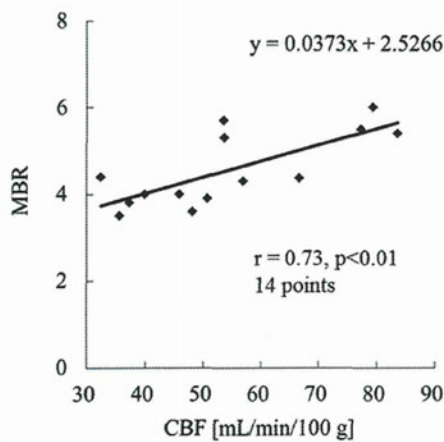


**Fig. 2.** Correlation between the absolute values of CBF and MBR at baseline. CBF and MBR were obtained by the hydrogen gas clearance method and LSF<sub>G</sub>, respectively. Each point represents 1 of 14 different rabbits. Correlation coefficient ( $r$ ) was 0.73 ( $P < 0.01$ ).

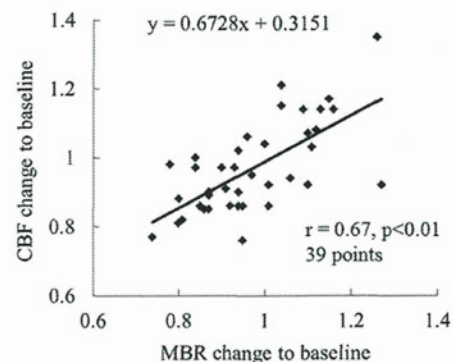


**Fig. 3.** Correlation between the relative changes in CBF and MBR after treatment with CO<sub>2</sub> and ET-1. Each point represents the ratio of relative values to baseline values. Total points were obtained from 39 time points ( $n = 9$  and 6 for CO<sub>2</sub> and ET-1, respectively) in 10 eyes of 14 rabbits. Correlation coefficient ( $r$ ) was 0.67 ( $P < 0.01$ ).

**Table 1**

Distributions of variances by randomized block ANOVA regarding individuality and time-course changes after each treatment.

Treatment	Individuality		Time-course changes	
	CBF	MBR	CBF	MBR
CO <sub>2</sub>	569.268 (8)*	15.046 (8)*	68.750 (3)*	1.358 (3)*
ET-1	262.346 (5)*	1.834 (5)*	11.056 (2)	0.127 (2)

Asterisks represent significant differences ( $P < 0.05$ ) among values obtained from individual rabbits or values at different time points. Degrees of freedom were shown in parentheses.

## 2.2. Measurement of CBF in ONH

Mydriasis was induced by topical tropicamide (Mydrin<sup>®</sup>-M ophthalmic solution 0.4%, Santen Pharmaceutical Co. Ltd., Osaka, Japan). Animals were anesthetized by intraperitoneal injection of 0.8 mg/kg urethane at 0.4 g/mL (Nakalai, Kyoto, Japan) and additional intramuscular injection of 0.1 mg/kg urethane as necessary. Topical anesthesia was induced by topical oxybuprocaine (Benoxil<sup>®</sup> ophthalmic solution 0.4%, Santen Pharmaceutical Co. Ltd.). The CBF in the ONH was measured by the hydrogen gas clearance method as previously reported (Sugiyama et al., 1996). A hydrogen electrode (Cat.# OA211-013, platinum needle with a 0.7-mm long and 0.1-mm diameter Pt–Ir tip, Unique Medical Co., Ltd., Tokyo, Japan) was inserted into a lower portion of the ONH with no visible surface vessels through the vitreous body from the pars plana using a vitrectomy lens. The reference electrode was subcutaneously fixed on the head. After the inhalation of 10% hydrogen gas by a mask at 5 L/min for 5 min, CBF was calculated with the hydrogen concentration half-life ( $T_{1/2}$ ) using a hydrogen clearance flow meter (model MDH-D1, Unique Medical Co., Ltd.). As shown in Fig. 1A, since the clearance curve is approximately mono-exponential, the hydrogen concentration was plotted into logarithm to get half-life ( $T_{1/2}$ ) for calculation. Specifically in the current study, the linearity of hydrogen clearance in logarithm was found beforehand to be the highest at 1–2 min after stopping hydrogen inhalation (Fig. 1B), therefore we adopted the half-life there to calculate CBF as  $69.3/T_{1/2}$  (mL/min/100 g).

## 2.3. Measurement method of MBR in ONH

MBR was measured with a LSFG-NAVI-MRC<sup>™</sup> device (Softcare Ltd., Iizuka, Japan). The LSFG-NAVI-MRC<sup>™</sup> consisted of a fundus camera equipped with a diode laser (wavelength: 830 nm) and a CCD image sensor (750 × 360 pixels). The principle and application of this method have been described previously (Konishi et al., 2002; Sugiyama et al., 2010; Tamaki et al., 1995). The measurement area of MBR was designated as a square area free of visible surface vessels near the hydrogen electrode in the ONH.

## 2.4. Measurements of CBF and MBR before and after altering ONH blood flow

To check their stability in measuring ONH blood flow, CBF and MBR were recorded 3 times at 15-min intervals and 5 times at 5-min intervals, respectively. The intervals were recommended in

previous reports (Sugiyama and Azuma, 1995; Tamaki et al., 1995). The inclusion criterion for the stability of measurements was a coefficient of variance (CV) of CBF within 0.1. Averages of measurement values were adopted as baseline values. The correlation between the baseline values of CBF and MBR was estimated. Baseline values were measured before the inhalation of carbon dioxide (CO<sub>2</sub>) or intravenous administration of endothelin-1 (ET-1).

Immediately, 15, and 30 min after 5-min inhalation of 10% CO<sub>2</sub> in ordinary air via mask at 5 L/min, CBF and MBR were measured simultaneously in the same rabbit. CBF was measured once at each time point. MBR was recorded 5 times at each time point, and then the mean value was calculated. Human ET-1 (Peptide Institute, Osaka, Japan) was dissolved in 0.1% aqueous acetic acid to provide a  $10^{-4}$  mol/L concentration and diluted with saline for a  $10^{-6}$  mol/L solution. CBF and MBR were measured, as above, at 30 min and 1 h after intravenous injection ( $10^{-10}$  mol/kg) of the prepared ET-1 solution. The relative change in CBF and MBR was calculated by dividing by the baseline value. The expiratory CO<sub>2</sub> density and arterial O<sub>2</sub> and CO<sub>2</sub> pressure were not monitored.

## 2.5. Statistical analysis

Correlation analysis between CBF and MBR was performed using Ekuseru-Toukei 2008 statistical software (Social Survey Research Information Co., Ltd., Tokyo, Japan). We analyzed the effects of each treatment (namely, CO<sub>2</sub> and ET-1) on MBR and CBF by randomized block ANOVA with individual animals as a block using JMP software (Ver. 9.0.0, SAS Institute, Cary, NC). Findings of  $P < 0.05$  were considered significant.

## 3. Results

### 3.1. Correlation between the baseline values of CBF and MBR

A plot of baseline CBF and MBR values is shown in Fig. 2. In 17 of 18 rabbits, the CV of CBF was within 0.1. For measurement of MBR in 3 of 17 rabbits, the square area could not be designated free from visible surface vessels near the hydrogen electrode in the ONH. Therefore, data from 14 eyes of 14 rabbits were used for this analysis. CBF and MBR were measured in the range (mean ± SE) of 32.4–83.5 ( $54.3 \pm 4.5$ ) mL/min/100 g and 3.5–6.0 ( $4.6 \pm 0.2$ ), respectively. A significant positive correlation between the absolute CBF and MBR baseline values was observed ( $r = 0.73$ ,  $P < 0.01$ ,  $n = 14$ ).

### 3.2. Correlation between the relative change in CBF and MBR induced by inhalation of CO<sub>2</sub> and intravenous administration of ET-1

CBF was altered after inhalation of CO<sub>2</sub> or intravenous administration of ET-1. Relative values of CBF changed in the range of 0.74–1.27. MBR in the ONH was also altered. Relative values of MBR changed in the range of 0.76–1.35. A plot of relative changes in CBF and MBR is shown in Fig. 3. In 10 of 14 rabbits, the changes in CBF and MBR induced by CO<sub>2</sub> ( $n = 9$ ) and ET-1 ( $n = 6$ ) were measured with the hydrogen gas clearance method and LSFG, respectively. The relative changes in CBF and MBR demonstrated a significant positive correlation ( $r = 0.67$ ,  $P < 0.01$ ).

**Table 2**

Average changes in CBF and MBR after inhalation of CO<sub>2</sub>.

	Baseline levels	Immediately	15 min	30 min
CBF (mL/min/100 g)	50.7 ± 11.5	52.3 ± 12.1 (1.04 ± 0.11)	48.3 ± 14.2 (0.95 ± 0.14)	46.0 ± 11.4* (0.91 ± 0.10)
MBR	4.7 ± 2.0	5.0 ± 2.0* (1.08 ± 0.10)	4.6 ± 2.5 (0.97 ± 0.13)	4.0 ± 1.4* (0.89 ± 0.08)

Data are expressed as mean ± SD for 9 rabbits. Asterisks represent significant differences ( $P < 0.05$ ) compared to baseline levels by paired *t*-test. CBF/MBR changes to baseline levels were shown in parentheses.